## Rugged spin-polarized electron sources based on negative electron affinity GaAs photocathode with robust Cs<sub>2</sub>Te coating

Cite as: Appl. Phys. Lett. 112, 154101 (2018); https://doi.org/10.1063/1.5026701 Submitted: 22 February 2018 . Accepted: 24 March 2018 . Published Online: 09 April 2018

Jai Kwan Bae 🗓, Luca Cultrera 🗓, Philip DiGiacomo, and Ivan Bazarov







## **ARTICLES YOU MAY BE INTERESTED IN**

Record-level quantum efficiency from a high polarization strained GaAs/GaAsP superlattice photocathode with distributed Bragg reflector

Applied Physics Letters 109, 252104 (2016); https://doi.org/10.1063/1.4972180

Monte Carlo simulations of electron photoemission from cesium antimonide Journal of Applied Physics 121, 215702 (2017); https://doi.org/10.1063/1.4984263

Monte Carlo charge transport and photoemission from negative electron affinity GaAs photocathodes

Journal of Applied Physics 113, 104904 (2013); https://doi.org/10.1063/1.4794822







## Rugged spin-polarized electron sources based on negative electron affinity GaAs photocathode with robust Cs<sub>2</sub>Te coating

Jai Kwan Bae, Luca Cultrera, Philip DiGiacomo, and Ivan Bazarov Cornell Laboratory for Accelerator-Based Sciences and Education, Cornell University, Ithaca, New York 14853, USA

(Received 22 February 2018; accepted 24 March 2018; published online 9 April 2018)

Photocathodes capable of providing high intensity and highly spin-polarized electron beams with long operational lifetimes are of great interest for the next generation nuclear physics facilities like Electron Ion Colliders. We report on GaAs photocathodes activated by  $Cs_2Te$ , a material well known for its robustness. GaAs activated by  $Cs_2Te$  forms Negative Electron Affinity, and the lifetime for extracted charge is improved by a factor of 5 compared to that of GaAs activated by Cs and  $O_2$ . The spin polarization of photoelectrons was measured using a Mott polarimeter and found to be independent from the activation method, thereby shifting the paradigm on spin-polarized electron sources employing photocathodes with robust coatings. *Published by AIP Publishing*. https://doi.org/10.1063/1.5026701

As of today, the operational lifetime of GaAs-based photocathodes remains a primary limit to the production of highly spin-polarized electron beams with high average currents. Such beams are essential to reach design luminosity for future facilities, such as the Electron Ion Collider, aimed at studying a wide range of phenomena from strong and electro-weak interactions to physics beyond the Standard Model. 4-4

Almost all electron sources for highly spin-polarized electron beams in accelerator physics rely on photocathode materials based on GaAs technology. By exposing the GaAs surface to a small quantity of cesium and an oxidant (oxygen or NF<sub>3</sub> gases are commonly used),<sup>5</sup> a strong dipole moment is formed at the surface that decreases the potential barrier of the electron emission into the vacuum. If the GaAs is also p-doped, due to downward pinning of the bands near the surface, the vacuum level can be lowered below the GaAs conduction band minimum (CBM) achieving the so called Negative Electron Affinity (NEA). When the NEA condition is reached, electrons that have relaxed to the bottom of the conduction band can still escape into the vacuum when they reach the surface. Such condition of GaAs results in a high Quantum Efficiency (QE) even for electrons that are excited with photon energies slightly larger than the band gap.<sup>6</sup>

The generation of spin-polarized photoelectrons from GaAs takes advantages of the selection rule which conserves the total angular momentum during transitions from the valence band to the conduction band. Due to the degeneracy of the heavy-hole and light-hole band in the P<sub>3/2</sub> valence band state, a bulk GaAs can provide up to 50% degree of polarization depending on the doping density.<sup>7</sup> Several approaches have been considered to increase the degree of electron spin polarization, the most effective being implementation of a lattice strain in GaAs aimed at breaking the energy degeneracy of the light and the heavy hole bands. Indeed, strained GaAs layers grown on GaAsP produce high polarization up to 90% by splitting the degenerate energy levels at a cost of decreased QE (0.07%) using a photon energy of 1.48 eV.<sup>8</sup> Very recently, GaAs/GaAsP multi-layer

super-lattices with a distributed Bragg reflector structure successfully showed an enhanced QE of 6.4% with a high polarization of 84%.<sup>9</sup>

NEA GaAs photocathodes are notorious for their exceptional vacuum sensitivity. Because activation layers are extremely vulnerable to chemical reactions and weakly bound to the bulk, they require extreme high vacuum (XHV) conditions to survive a long enough time to be of any practical use. Mainly three mechanisms are responsible for the surface degradation of GaAs activated to NEA: ion back-bombardment, <sup>10</sup> chemical poisoning,11 and thermal desorption of the activation layer. 12 The degradation of photocathode lifetime due to ion back-bombardment is proportional to the overall charge extracted from the cathode. It can be mitigated by extracting electrons from a spot several mm off the electrostatic center of the electron gun. 10 The advantages of operating under such experimental conditions have been demonstrated in the case of GaAs as well as alkali antimonides. 13,14 When NF<sub>3</sub> is used as an oxidant, it was reported that activation performed using Cs and Li simultaneously can lead to improved lifetimes. 15,16 These studies suggest that chemically stable activation layers can enhance operational lifetime and improve photocathode's ability to better withstand both ion back-bombardment and chemical poisoning.

Cs<sub>2</sub>Te is a well known solar-blind photocathode material. Its resistance to chemical poisoning and poor vacuum conditions is much larger than that of GaAs. Therefore, it is the most commonly used high-QE photocathode in normal conducting RF guns known for their poorer vacuum.<sup>17</sup> Recent studies showed that Cs<sub>2</sub>Te can also form NEA on GaAs due to a peculiar alignment of the electronic bands of the two materials as shown in Fig. 1.<sup>18–20</sup>

In this work, we report a NEA condition produced on bulk GaAs using a  $Cs_2Te$  activation layer, the polarization measurements, and the charge lifetime obtained for these photocathodes. Our results demonstrate a more stable NEA surface as compared to the traditional activation using Cs and  $O_2$ , without negatively affecting the spin polarization of photoemitted electrons.

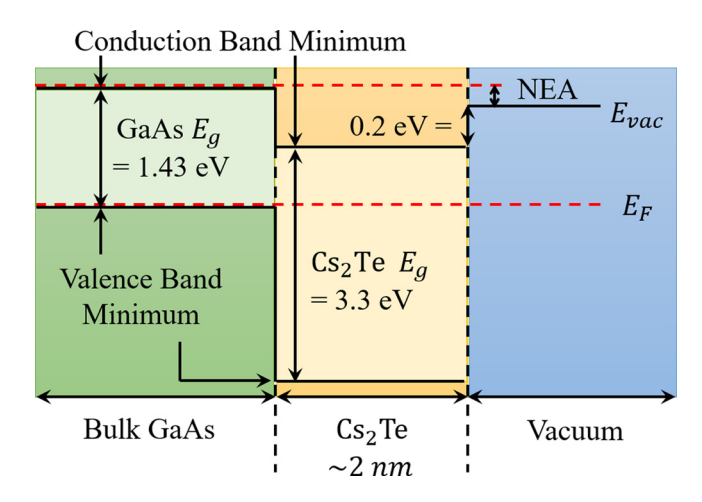


FIG. 1. Energy band diagram of GaAs with  $Cs_2Te$  activation layer. If near IR light ( $\sim$ 1.43 eV) is illuminating the sample, the photoelectrons are excited from the GaAs valence band because electrons in  $Cs_2Te$  require 3.5 eV to reach the vacuum level. NEA is formed on the surface because the vacuum level ( $E_{vac}$ ) is below the GaAs conduction band minimum.

Several different specimens were prepared from the same highly p-doped (Zn  $5 \times 10^{18} \text{ cm}^{-3}$ ) GaAs (100) wafer. In order to remove the native oxide layer, a wet etch was performed in a 4% HCl solution for 5 min under the hood in the air. Then, samples were rinsed in deionized water, dried using pure nitrogen, connected to the sample holder, and loaded under vacuum in less than 1 h. A mild sample heating at about 400 °C for 12 h was deemed sufficient to yield a surface clean enough to perform our experiments. This was inferred from observing that after heating, the samples could be activated to NEA using only Cs (photoemission observed with  $\sim 1.43 \, \text{eV}$  photons). The growth of Cs<sub>2</sub>Te was performed in a ultra-high vacuum (UHV) chamber equipped with effusion cells hosting BN crucibles loaded with Cs (99.5% from Strem Chemicals) and Te (99.999% from Sigma-Aldrich). Each source is equipped with a shutter that allows to trigger on and off the flux towards the substrate surface. After the heat cleaning, the temperature of the samples was lowered to approximately 130 °C, and the light of a small diode laser operating at 532 nm was used to illuminate the negatively biased photocathode surface. The Cs<sub>2</sub>Te growth on GaAs was performed while continuously cooling down the sample from the initial temperature of about 130 °C [see Fig. 2(c)]. Initially [see Figs. 2(a) and 2(b)], only a small flux of Cs was evaporated until the photocurrent is saturated for an equivalent QE of about 0.5%, which demonstrates sufficient cleanliness of the GaAs surface. At this point, the shutter for Cs was closed and the one for Te was opened. A sharp decrease in the photocurrent was observed, followed by deposition of 0.5 nm thick Te layer as estimated from the quartz microbalance frequency shift [Fig. 2(b)]. Another Cs deposition followed. The photocurrent increased again until an equivalent QE of about 1% was reached. Subsequent simultaneous evaporation of Cs and Te (which adds the equivalent of another 0.5 nm of Te) did not improve QE much further [Figs. 2(a) and 2(b)]. Upon final cooling down, the samples were exposed to a very small flux of Cs reaching a typical final QE of about 1.5% at 532 nm.

One of the samples was moved under UHV into our surface analysis chamber to analyze the surface by collecting

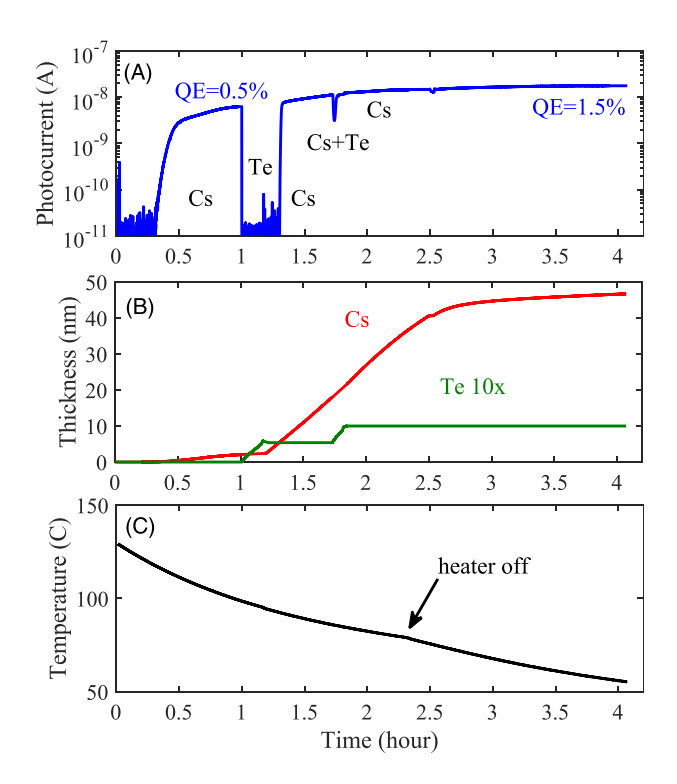


FIG. 2. (a) Photocurrent measured over time with a 532 nm laser illuminating GaAs during alternating exposure to Cs and Te evaporation; (b) estimated thicknesses of Cs and Te from the quartz microbalance frequency shift; (c) GaAs substrate temperature during the growth of  $Cs_2Te$ .

the Auger spectrum (Fig. 3). The Auger spectra clearly show the distinctive peaks of Te and Cs confirming the presence of the two elements over the GaAs surface. Detection of Auger electrons from Ga and As also confirms that the Cs and Te layers are only few nm thick.

The NEA condition was experimentally verified from the spectral response measurements of QE using a broadband lamp and a monochromator. Figure 4 shows a typical spectral response from one of our GaAs samples activated with Cs<sub>2</sub>Te, comparing it with a similar result reported in literature.<sup>20</sup> The photoemission at the photon energy of 1.43 eV (the band gap of GaAs) supports the conclusion that the NEA condition is achieved at the surface.

Two different metrics are often used for lifetime of a photocathode: operational lifetime, defined as the amount of

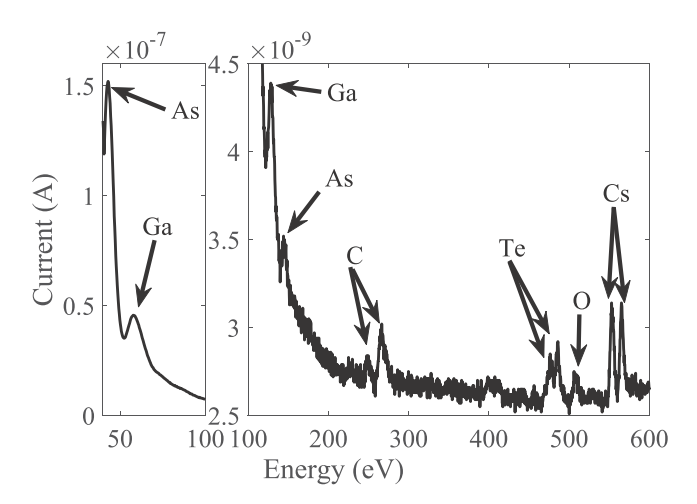


FIG. 3. Auger electron spectra of GaAs with Cs<sub>2</sub>Te activation layer.

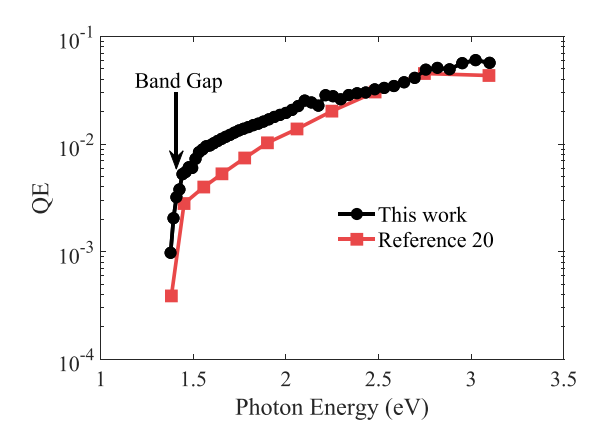


FIG. 4. Typical spectral response of our  $GaAs-Cs_2Te$  as compared to the one from Ref. 20.

time a photocathode can satisfy the QE requirement for a particular purpose, and charge lifetime, defined as the amount of charges extracted until QE drops to 1/e of the initial value. 10 The latter has been suggested as a more appropriate figure of merit when comparing the performance of different photocathodes. In Fig. 5, all lifetime measurements were performed under very similar vacuum conditions (better than  $1 \times 10^{-10}$  Torr) using a 532 nm laser light excitation  $(\sim 50 \,\mu\text{W})$  with identical spot size for all illuminations. After each Cs<sub>2</sub>Te growth, the photocurrent of each sample was constantly measured until the QE went to the  $1 \times 10^{-3}$  level or below. Once such level was reached, the samples were exposed to a Cs flux using alkali-chromate-based dispensers to restore the initial efficiency. QEs were monitored also for the recesiated samples, and all the results are reported in Fig. 5.

The sample coated with an activation layer grown with a 1.2-nm thin film of Te showed the largest charge lifetime value of  $9.4 \times 10^{-3}$  C. At the same time, the QE at 532 nm was measured to be a factor of 2 larger than the one obtained when a 1.0-nm Te thin film was used. Compared to the lifetime of  $1.9 \times 10^{-3}$  C measured for a GaAs activated with Cs and  $O_2$ , the  $Cs_2$ Te layer enhanced the lifetime by a factor of 5 in our experimental conditions. While the exposure to Cs vapors was effective in restoring QEs to even higher levels

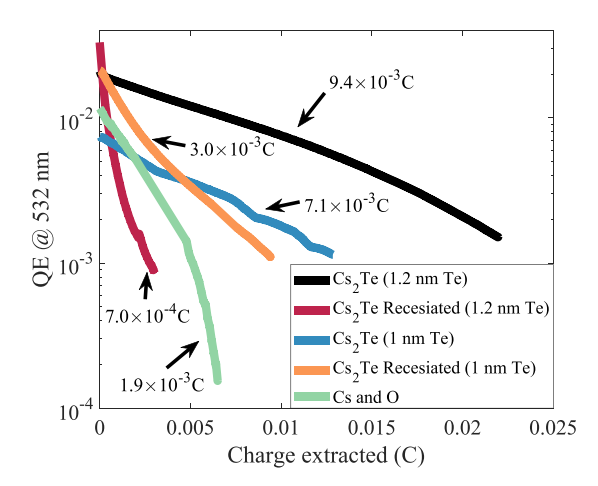


FIG. 5. Quantum efficiency of GaAs with various surface conditions at 532 nm wavelength as a function of extracted charges. The number next to each curve is the charge lifetime obtained from an exponential fit.

than the original ones, the charge lifetimes of the recesiated samples are considerably shorter than the original ones. The recesiated samples had charge lifetimes comparable to those of the Cs and  $O_2$  activated ones. This seems to suggest that Cs atoms did not penetrate deeply and/or react with the  $Cs_2Te$  layer but rather deposited on the surface after the recesiation.

Despite the fact that our experiments were performed under UHV conditions, all the charge lifetimes that were measured appear orders of magnitude lower than those reported for GaAs activated to NEA that operated in one of the CEBAF electron guns with a beam energy of 100 keV.<sup>21</sup> A simple explanation to this experimental result is related to the vastly different experimental conditions we had in our case. Indeed, unlike the CEBAF gun where the electron beam is accelerated to 100 keV, photoelectrons in our setup are accelerated to mere ~40 eV. At such low kinetic energies, the electron impact ionization cross-section for molecular hydrogen (which is considered to be the dominant chemical species in the residual gas of the vacuum chamber) is 3 orders of magnitude greater than that at 100 keV. 10,21 Also, due to the lack of any deflecting fields, electrons and ions trajectories are co-linear, so that the flux of back-streaming ions is likely to impact at the exact location where the laser spot is illuminating the photocathode. Finally, the positive ions are accelerated at relatively low energies, and hence they will mostly damage a very shallow region near the surface rather than penetrating deeper into the bulk, i.e., affecting the layers responsible for the NEA more effectively.

The photocathode laboratory UHV installation has been upgraded with a low energy reflection mode Mott polarimeter that was originally part of SLAC photocathode test-stand. This Mott analyzer's Sherman function was characterized to be  $S_{\rm eff}=0.15$  at  $20\,\rm kV$  operating voltage with a 5% accuracy when electrons within a  $1\,\rm keV$  energy loss window are allowed to be detected. Monochromatic light was circularly polarized using a linear polarizer (Thorlabs LPVIS050) and a liquid crystal variable wave plate (Thorlabs LC1113B), and it was directed unto the sample surface at normal incidence. The helicity of circular polarization was switched by alternating retardance of the liquid crystal wave plate between  $\frac{1}{4}\lambda$  and  $\frac{3}{4}\lambda$ .

One of GaAs samples was first activated to NEA using Cs and O<sub>2</sub>, and then moved into the UHV chamber equipped with the Mott polarimeter. Photoelectrons were transported to the Mott detector, and from the measured asymmetries in the scattering process and the known value of the  $S_{\rm eff}$ , the electron beam polarization was obtained for different wavelengths (see Fig. 6). The measured values agree well with those recently reported for similar bulk GaAs by another group. The same sample was then moved back to the Cs2Te growth chamber. There it was first heated for 12 h at 400 °C to remove the Cs and O<sub>2</sub> from its surface, and then Cs<sub>2</sub>Te thin film was deposited on it. Once the GaAs sample was activated with Cs<sub>2</sub>Te, it was moved back to the Mott chamber to measure the spin polarization of photoelectrons. Results are reported in Fig. 6 as well. We found that the Cs2Te thin film did not affect the polarization of the photoelectrons from GaAs.

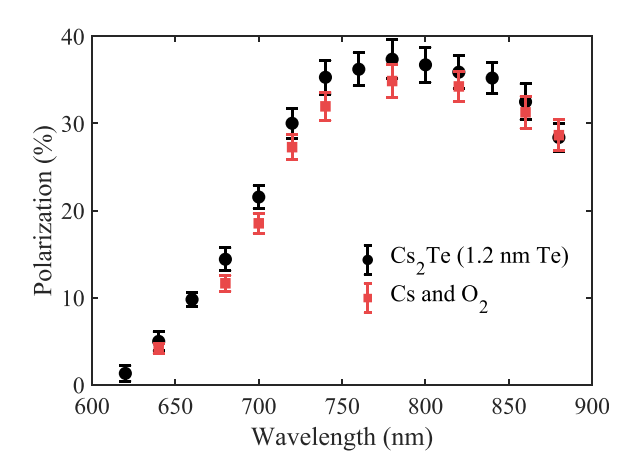


FIG. 6. Spin polarization measured from GaAs samples activated by  $Cs_2Te$  and Cs and  $O_2$  as a function of the laser wavelength.

Although the maximum theoretical electron spin polarization achievable for bulk GaAs is 50%, due to spin relaxation mechanisms happening before the emission into vacuum, 30%-40% degree of polarization is usually attained from NEA GaAs. For GaAs, electron spin relaxation mechanisms have been extensively studied and are dominated by the lack of inversion symmetry and the exchange interaction between electrons and holes, leading to a characteristic relaxation time  $\tau_s$  of  $\sim$ 100 ps at room temperature. <sup>24–26</sup> Additional depolarization mechanisms at activation layers are relatively unknown and have been considered negligible because the Cs and O<sub>2</sub> activation is on the order of less than a monolayer. In case of Cs<sub>2</sub>Te activation layer, the thickness might be no longer negligible and the activation layer can become an additional source of spin depolarization. Based on Refs. 25 and 26, we estimate  $\tau_s$  to be similar to that of GaAs but dominated by the lack of inversion symmetry and the spin-orbit coupling, due to a heavier electron effective mass. The conduction band electron effective mass of  $1.1m_e$  at  $\Gamma$  point was used based on calculations.<sup>27</sup> From this estimate, we expect that electrons can travel several tens of nm in Cs<sub>2</sub>Te without experiencing significant depolarization. Our results reported in Fig. 6 support this conclusion.

An electron mean free path of 3 nm and mean energy losses of 5 meV have been used to accurately reproduce the spectral response of  $Cs_2Te$  using Monte Carlo techniques. Assuming 0.15 eV as the maximum energy of electrons excited in GaAs with 780 nm light and injected into the  $Cs_2Te$  layer (see Fig. 1), electrons should still be able to escape even after having experienced on the order of 30 (= 0.15 eV/5 meV) scattering events. Making the assumption of small scattering angles,  $^{29}$  a few tens of nm of  $Cs_2Te$  should also not drastically affect the efficiency of electron emission.

In conclusion, we activated GaAs with Cs<sub>2</sub>Te for studying its effect on NEA formation, lifetime, and spin-polarization of the photocathode. NEA condition was confirmed by the spectral response. The lifetime showed a factor of 5 improvement while the spin polarization remained the same as the one obtained with the Cs and O<sub>2</sub> standard activation. Based on our presented results and simplified estimates predicting negligible losses of quantum efficiency and spin

polarization, we plan to experiment with a thicker Cs<sub>2</sub>Te to further improve the photocathode lifetime. We believe that our work triggers a paradigm shift on activating GaAs photocathodes with other materials that can both form more robust NEA activation layers and enable applications requiring high spin-polarized photoelectrons.

This work was supported by DOE Grant Nos. DE-SC0016203 and NSF PHY-1461111. The authors wish to acknowledge T. Maruyama, M. Stuzman, and M. Poelker for fruitful discussions and help in recommissioning the Mott polarimeter.

<sup>1</sup>See https://science.energy.gov/~/media/np/pdf/Reports/Report\_of\_the\_ Community\_Review\_of\_EIC\_Accelerator\_RD\_for\_the\_Office\_of\_Nuclear\_ Physics\_20170214.pdf for "Report of the Community Review of EIC Accelerator R&D for the Office of Nuclear Physics" (last accessed February 19, 2018).

<sup>2</sup>See http://science.energy.gov/~/media/np/nsac/pdf/2015LRP/2015\_LRPNS\_091815.pdf for "The 2015 Long Range Plan for Nuclear Science" (last accessed February 19, 2018).

<sup>3</sup>See https://science.energy.gov/~/media/np/nsac/pdf/docs/2013/NSAC\_FacilitiesReport.pdf for "Major Nuclear Physics Facilities for the Next Decade: Report of the NSAC Subcommittee on Scientific Facilities" (last accessed March 24, 2018).

<sup>4</sup>J. McCarter, A. Afanasev, T. Gay, J. Hansknecht, A. Kechiantz, and M. Poelker, Nucl. Instrum. Methods Phys. Res. Sect. A **738**, 149 (2014).

<sup>5</sup>F. Ciccacci and G. Chiaia, J. Vac. Sci. Technol. A 9, 2991 (1991).

<sup>6</sup>D. T. Pierce, R. J. Celotta, G. C. Wang, W. N. Unertl, A. Galejs, C. E. Kuyatt, and S. R. Mielczarek, Rev. Sci. Instrum. **51**, 478 (1980).

<sup>7</sup>W. Liu, M. Poelker, X. Peng, S. Zhang, and M. Stutzman, J. Appl. Phys. 122, 035703 (2017).

<sup>8</sup>T. Maruyama, E. L. Garwin, R. Prepost, and G. H. Zapalac, Phys. Rev. B 46, 4261 (1992).

<sup>9</sup>W. Liu, Y. Chen, W. Lu, A. Moy, M. Poelker, M. Stutzman, and S. Zhang, Appl. Phys. Lett. **109**, 252104 (2016).

<sup>10</sup> J. Grames, R. Suleiman, P. A. Adderley, J. Clark, J. Hansknecht, D. Machie, M. Poelker, and M. L. Stutzman, Phys. Rev. Spec. Top.-Accel. Beams 14, 043501 (2011).

<sup>11</sup>N. Chanlek, J. D. Herbert, R. M. Jones, L. B. Jones, K. J. Middleman, and B. L. Militsyn, J. Phys. D: Appl. Phys. 47, 055110 (2014).

<sup>12</sup>M. Kuriki, C. Shonaka, H. Iijima, D. Kubo, H. Okamoto, H. Higaki, K. Ito, M. Yamamoto, T. Konomi, S. Okumi, M. Kuwahara, and T. Nakanishi, Nucl. Instrum. Methods A 637, S87 (2011).

<sup>13</sup>L. Cultrera, J. Maxson, I. Bazarov, S. Belomestnykh, J. Dobbins, B. Dunham, S. Karkare, R. Kaplan, V. Kostroun, Y. Li, X. Liu, F. Löhl, K. Smolenski, Z. Zhao, D. Rice, P. Quigley, M. Tigner, V. Veshcherevich, K. Finkelstein, D. Dale, and B. Pichler, Phys. Rev. Spec. Top.-Accel. Beams 14, 120101 (2011).

<sup>14</sup>R. R. Mammei, R. Suleiman, J. Feingold, P. A. Adderley, J. Clark, S. Covert, J. Grames, J. Hansknecht, D. Machie, M. Poelker, T. Rao, J. Smedley, J. Walsh, J. L. Mccarter, and M. Ruiz-Osés, Phys. Rev. Spec. Top.-Accel. Beams 16, 033401 (2013).

<sup>15</sup>Y. Sun, R. E. Kirby, T. Maruyama, G. A. Mulhollan, J. C. Bierman, and P. Pianetta, Appl. Phys. Lett. 95, 174109 (2009).

<sup>16</sup>G. A. Mulhollan and J. C. Bierman, J. Vac. Sci. Technol. A 26, 1195 (2008).

<sup>17</sup>P. Michelato, L. Monaco, C. Pagani, D. Sertore, and F. Stephan, in Proceedings of EPAC08, Genoa, Italy, 2008.

<sup>18</sup>H. Sugiyama, K. Ogawa, J. Azuma, K. Takahashi, M. Kamada, T. Nishitani, M. Tabuchi, T. Motoki, K. Takashima, A. Era, and Y. Takeda, J. Phys.: Conf. Ser. 298, 012014 (2011).

<sup>19</sup>K. Uchida, M. Kuriki, Y. Seimiya, R. Kaku, K. Miyoshi, and N. Yamamoto, in Proceedings of IPAC2014, Dresden, Germany, 2014.

<sup>20</sup>M. Kuriki, S. Kashiwagi, Y. Seimiya, and K. Uchida, in Proceedings of IPAC2015, Richmond, VA, USA, 2015.

<sup>21</sup>C. K. Sinclair, P. A. Adderley, B. M. Dunham, J. C. Hansknecht, P. Hartmann, M. Poelker, J. S. Price, P. M. Rutt, W. J. Schneider, and M. Steigerwald, Phys. Rev. Spec. Top.-Accel. Beams 10, 023501 (2007).

- <sup>22</sup>R. Alley, H. Aoyagi, J. Clendenin, J. Frisch, C. Garden, E. Hoyt, R. Kirby, L. Klaisner, A. Kulikov, R. Miller *et al.*, Nucl. Instrum. Methods Phys. Res. Sect. A 365(1), 1–27 (1995).
- <sup>23</sup>G. A. Mulhollan, "Low-energy polarized electron source test facilities," SLAC Report No. SLAC-REPRINT-1994-081, 1994.
- <sup>24</sup>G. Fishman and G. Lampel, Phys. Rev. B **16**, 820 (1977).
- <sup>25</sup>I. Zutic, J. Fabian, and S. D. Sarma, Rev. Mod. Phys. **76**, 323 (2004).
- <sup>26</sup>P. H. Song and K. W. Kim, Phys. Rev. B **66**, 035207 (2002).
- <sup>27</sup>J. Z. Terdik, K. Németh, K. C. Harkay, J. H. Terry, L. Spentzouris, D. Velázquez, R. Rosenberg, and G. Srajer, Phys. Rev. B 86, 035142 (2012).
- <sup>28</sup>G. Ferrini, P. Michelato, and F. Parmigiani, Solid State Commun. 106, 21 (1998).
- <sup>29</sup>C. Jacoboni and P. Lugli, *The Monte Carlo Method for Semiconductor Device Simulation* (Springer Verlag, 1989), p. 48.